

Supporting Online Material

Type II Detwinning in NiTi

Tawhid Ezaz and Huseyin Sehitoglu*

Department of Mechanical Science and Engineering, University of Illinois,
1206 West Green Street, Urbana, IL 61801

* To whom correspondence should be addressed. Email: huseyin@illinois.edu

This PDF file includes

Materials and Methods

Table I and II

Supplementary references

Figs. 1 and 2

Materials and Methods

Lattice parameter in B19' and first principle total energy calculations are performed using Density functional theory based Vienna ab-initio Simulation Package (VASP) ¹ and the generalized gradient approximation (GGA) ² is implemented on a projection augmented wave (PAW) . PAW GGA potential implemented by Perdew et al. considers even s-orbitals of Ti as valence and is utilized in current study. Monkhorst-Pack ³ 9 x 9 x 9 *k*-point meshes are used for Brillouin zone integration. Spin polarization and an energy cut-off of 350 eV is maintained for all calculations. During strain controlled deformation, only ion positions are relaxed and both volume and shape of the simulation box are held constant ensuring the correct monoclinic angle. Ionic relaxation is performed using conjugate gradient algorithm. The electronic convergence threshold was maintained at 10⁻⁶ eV per unit cell for structural relaxation and deformed states. Tolerance values for internal forces are set to be 10⁻³ eVÅ⁻¹.

In NiTi, B19' martensite has a monoclinic structure with a space group P2₁/m. The structural parameter and the total energy relative to B2 phase is given in Table I. The ground-state structures agree very well with experimental data⁴ as shown in supplementary Table I. The stable energy corresponding to the lattice parameter is computed and compared with NiTi B2 structure. The magnitude indicates that, B19' phase is lower in energy than B2 phase by 0.04899 eV and hence energetically more stable. The stable energy differences are in agreement with reported values by Huang et. al⁵. The agreement of structural and energetic data ensures our calculations are well converged.

The DFT calculations for GPFE are conducted using a 9 layer supercell having 8-atoms per layer. Periodic boundary conditions are maintained across the supercell to represent bulk NiTi martensite (no free surface). A 1 layer twin is created by sliding the layers 3-9 relative to layers 1 to 2 along [011] direction through a displacement $\bar{b} \approx 1/9[011]$ in the (111) plane ensuring a shear

magnitude of 0.28040. Here, we note that, NiTi in martensite has a monoclinic structure and can be expressed with three lattice constants a, b, c and a monoclinic angle β (magnitude of lattice constants are given in Supplementary Table I). Therefore, vector length with Miller index $[011]$ essentially corresponds to a length of $[0\ b\ c]$, where b and c are the martensite lattice constants in $[010]$ and $[001]$ directions respectively. A 2-layer twin is, then, generated by sliding layers 4-9 in similar fashion; 3-layer twin by sliding layers 5-9 and so on. The shear deformation secures correct position of a Type II twin for Ti atoms.

We allowed complete relaxation of Ni atoms during energy minimization calculations whereas Ti atoms are only partially relaxed normal to the shear direction. During shearing of the supercell, primitive vectors are adjusted which maintain the correct stacking between the adjacent supercell ensuring the periodicity. This similar procedure has been described in early work⁶.

Table I

<i>Structure</i>	<i>a</i> (Å)	<i>b</i> (Å)	<i>c</i> (Å)	β (°)	V_0 (Å ³)	$E - E_{B2}$ (eV)
B19' (present)	2.884	4.11	4.6649	97.8	27.39	-0.04899
B19' (Exp) ^a	2.898	4.108	4.646	97.8	27.4	
B19' ^b	2.892	4.049	4.598	97.8	26.67	-0.046

^a Reference ⁴

^b Reference ⁵

Table II

<i>Atoms</i>	<i>Shear plane</i>	<i>Shear direction</i>	<i>Shear magnitude s</i>	<i>Shuffle</i> (Å)	<i>Shuffle direction</i>
Ti	(1 1 $\bar{1}$)	[0 1 1]	0.28040	-	-
Ni	(1 1 $\bar{1}$)	[0 1 1]	0.28040	0.6385	[2 0 5] and [$\bar{2}$ 0 $\bar{5}$]

References

- ¹ G. Kresse and J. Hafner, *Physical Review B (Condensed Matter)* **48** (17), 13115 (1993).
- ² J. P. Perdew, K. Burke, and M. Ernzerhof, *Physical Review Letters* **77** (18), 3865 (1996).
- ³ H. J. Monkhorst and J. D. Pack, *Physical Review B (Solid State)* **13** (12), 5188 (1976).
- ⁴ Y. Kudoh, M. Tokonami, S. Miyazaki, and K. Otsuka, *Acta Metallurgica* **33** (11), 2049 (1985).
- ⁵ Huang Xiangyang, G. J. Ackland, and K. M. Rabe, *Nature Materials* **2** (5), 307 (2003).
- ⁶ S. Kibey, J. B. Liu, D. D. Johnson, and H. Sehitoglu, *Acta Materialia* **55** (20), 6843 (2007).

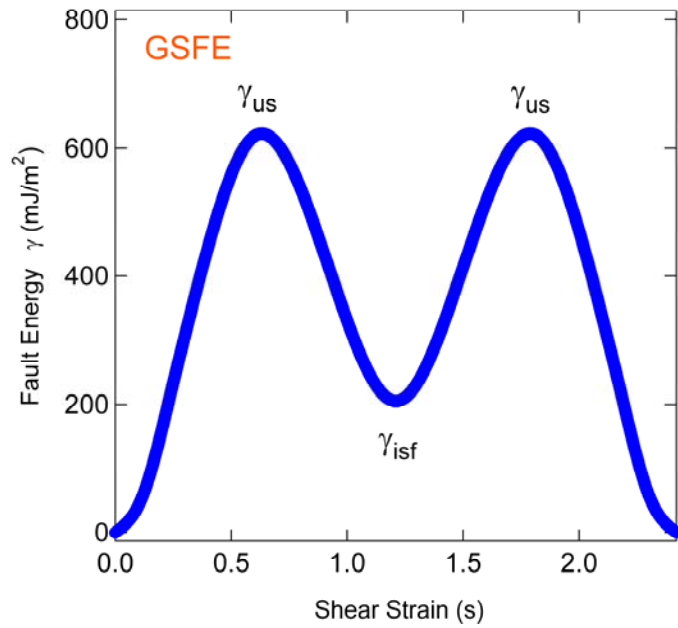


Fig. 1. Generalized stacking fault energy (GSFE) of NiTi martensite in $(11\bar{1})[011]$ system. Fault energy γ (mJ/m^2) is plotted against shear strain (s) to slide one elastic $(11\bar{1})$ plane against other in $[011]$ direction. Shear strain (s) is calculated from the displacement of top layer and interplanar distance between two $(11\bar{1})$ plane.

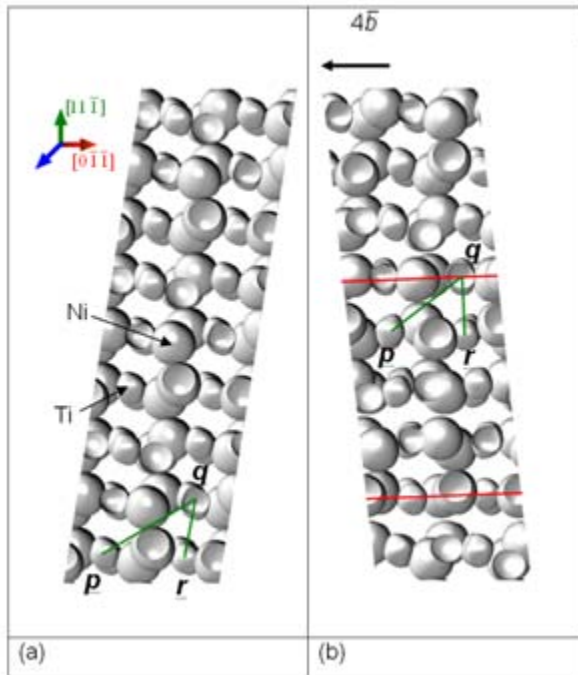


Fig. 2. Charge density isosurface of $0.50 \text{ eV} / \text{Å}^3$ in NiTi martensite after relaxation (a) at undeformed condition (b) with four layer twin. The cubic (spherical) structure shows the isosurface of the Ti (Ni) ions. Center of the isosurface points to the nucleus of the atom. The isosurface after deformation does not show any periodic stacking interaction in the simulation box. The green line p - q - r indicates the extracted path used for charge density in Ti-Ti interaction. Similar technique is utilized for Ni-Ni and Ni-Ti interactions.